



## pH-dependent Co(II) assemblies from achiral 2-benzothiazolythioacetic acid: crystal structures, symmetry breaking, and magnetic properties

Chun-Yue Shu, Fu-Ping Huang, Qing Yu, Peng-Fei Yao, He-Dong Bian, Ru-Qian Lan & Bei-Lei Wei

To cite this article: Chun-Yue Shu, Fu-Ping Huang, Qing Yu, Peng-Fei Yao, He-Dong Bian, Ru-Qian Lan & Bei-Lei Wei (2015) pH-dependent Co(II) assemblies from achiral 2-benzothiazolythioacetic acid: crystal structures, symmetry breaking, and magnetic properties, Journal of Coordination Chemistry, 68:12, 2107-2120, DOI: [10.1080/00958972.2015.1038996](https://doi.org/10.1080/00958972.2015.1038996)

To link to this article: <http://dx.doi.org/10.1080/00958972.2015.1038996>



Accepted author version posted online: 08 Apr 2015.  
Published online: 13 May 2015.



Submit your article to this journal [↗](#)



Article views: 89



View related articles [↗](#)



View Crossmark data [↗](#)

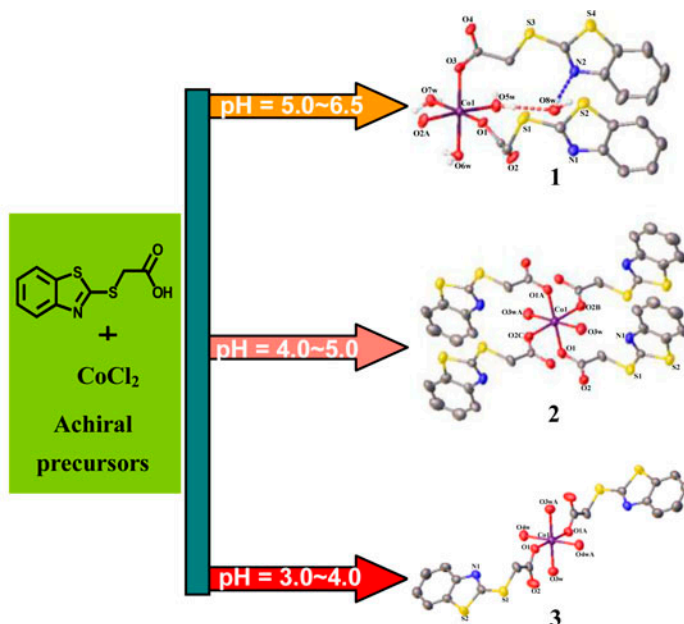
## pH-dependent Co(II) assemblies from achiral 2-benzothiazolythioacetic acid: crystal structures, symmetry breaking, and magnetic properties

CHUN-YUE SHU<sup>†</sup>, FU-PING HUANG\*<sup>†</sup>, QING YU<sup>†</sup>, PENG-FEI YAO<sup>†</sup>,  
HE-DONG BIAN<sup>‡</sup>, RU-QIAN LAN<sup>‡</sup> and BEI-LEI WEI<sup>†</sup>

<sup>†</sup>Key Laboratory for the Chemistry and Molecular Engineering of Medicinal Resources, School of Chemistry and Pharmaceutical Sciences, Ministry of Education of China, Guangxi Normal University, Guilin, PR China

<sup>‡</sup>School of Chemistry and Chemical Engineering, Guangxi University for Nationalities, Nanning, PR China

(Received 13 May 2014; accepted 18 March 2015)



Three Co(II) complexes, {[Co(L)<sub>2</sub>(H<sub>2</sub>O)<sub>3</sub>]·H<sub>2</sub>O}<sub>n</sub> (**1**), [Co(L)<sub>2</sub>(H<sub>2</sub>O)<sub>2</sub>]<sub>n</sub> (**2**), and [Co(L)<sub>2</sub>(H<sub>2</sub>O)<sub>4</sub>]·2H<sub>2</sub>O (**3**), were obtained under different pH (HL = achiral 2-benzothiazolythioacetic acid). Compound **1** was synthesized at pH 5.0–6.5 and possesses a chiral 1-D helical double chain structure, which achieved chiral symmetry breaking. Compound **2** was obtained at pH 4.0–5.0 and has a 1-D chain structure. Compound **3** was generated at pH 3.0–4.0 and is a mononuclear structure.

\*Corresponding author. Email: [huangfp2010@163.com](mailto:huangfp2010@163.com)

Based on an achiral 2-benzothiazolythioacetic acid (HL) ligand, three Co(II) coordination compounds,  $\{[\text{Co}(\text{L})_2(\text{H}_2\text{O})_3] \cdot \text{H}_2\text{O}\}_n$  (**1**),  $[\text{Co}(\text{L})_2(\text{H}_2\text{O})_2]_n$  (**2**), and  $[\text{Co}(\text{L})_2(\text{H}_2\text{O})_4] \cdot 2\text{H}_2\text{O}$  (**3**), were obtained under different pH environments. Compound **1** possessing an interesting chiral 1-D helical double chain was synthesized with pH of 5.0–6.5, and the chiral symmetry breaking has been probed by single-crystal X-ray diffraction and circular dichroism spectroscopy. Switching pH to 4.0–5.0 and 3.0–4.0 resulted in achiral **2** and **3**, respectively. Compound **2** has a 1-D chain structure and **3** is mononuclear.

*Keywords:* Crystal structure; Chiral symmetry breaking; Magnetic behavior

## 1. Introduction

Chiral compounds play an indispensable role in biological function and in many areas of society and science such as medicine, biology, biotechnology, chemistry, and materials science [1–4]. Of them, homochiral metal–organic coordination polymers have attracted interest owing to their potential applications in enantioselective separation, asymmetric catalysis, nonlinear optics, and sensor technology [5–8].

When discussing chirality in complexes, one needs to consider two different aspects [9]; first, whether the components (building blocks) of the structure are chiral themselves, and second, whether the arrangement of components into the complex is chiral. In general, we are very comfortable with such chirality coming from an asymmetric carbon or other so-called chiral centers and that's because using a chiral component as a starting point is the easiest way to 'design' a chiral complex [10].

However, chiral complexes from achiral building blocks are less common [11]. Chirality can be induced by coordination around the metal center (e.g. carboxyl, which can form a helical chain to generate chiral complex by *syn-anti* bridging), flexibility of the ligands, inter/intramolecular hydrogen bonds, stacking interactions, etc. [12]. In this case, statistically, left- and right-handed helical molecules should be of the same number, because each enantiomer should be formed with equal probability if no enantiopure additive or chiral physical environment is introduced [3c, 11b, 13], unless, spontaneous chiral symmetry breaking occurs, where the number of one enantiomer is not equal to that of the other. Just like flipping a coin, if we flip a coin a sufficient number of times, we can get the coin resting on either side with equal probability. However, if we limit the flipping to just a small number of events, the chance of getting just one particular side up becomes higher than the other side. Since the first realization reported by Kondepudi *et al.* [14], where  $\text{NaClO}_3$  crystallized in homochiral form from achiral precursors through chiral symmetry breaking, much attention has been paid to unusual phenomenon. Later, Wu *et al.* [15] achieved chiral symmetry breaking of  $[\{\text{Cu}(\text{succinate})(4,4'\text{-bipyridine})\}_n] \cdot (4\text{H}_2\text{O})_n$  by modulating the pH of the reaction and controlling the solution evaporation rate; Zheng *et al.* [11b] gained a homochiral coordination polymer  $\{\text{Ni}_{1.5}(\text{tzdc})(\text{H}_2\text{O})_3\} \cdot 3\text{H}_2\text{O}$  ( $\text{H}_3\text{tzdc} = 4\text{H}-1,2,4\text{-triazole-}3,5\text{-dicarboxylic acid}$ ) from achiral precursors, which could be driven by intrinsic chiral quartz topology; Qin *et al.* [16] also obtained a homochiral coordination polymer  $\{[\text{Co}(1,1'\text{-oxybis}(3,5\text{-dipyridinebenzene))}(\text{OBA})] \cdot (\text{H}_2\text{O})\}_n$  [ $\text{H}_2\text{OBA} = 4,4'\text{-oxybis}(\text{benzoate})$ ] from achiral precursors, which could be induced by flexibility of ligand and the introduction of co-ligand.

Herein, we report three different Co(II) complexes,  $\{[\text{Co}(\text{L})_2(\text{H}_2\text{O})_3] \cdot \text{H}_2\text{O}\}_n$  (**1**),  $[\text{Co}(\text{L})_2(\text{H}_2\text{O})_2]_n$  (**2**), and  $[\text{Co}(\text{L})_2(\text{H}_2\text{O})_4] \cdot 2\text{H}_2\text{O}$  (**3**), generated under different pH environments

based on an achiral ligand (2-benzothiazolythioacetic acid). The pH of 5.0–6.5 produced **1** which holds chiral 1-D helical double chains owing to the *syn-anti* bridging of carboxyl. In addition, the chiral symmetry has broken through an unusual spontaneous asymmetric crystallization by circular dichroism (CD) spectroscopy. When the pH was switched to 4.0–5.0 and 3.0–4.0, achiral **2** and **3** were obtained, respectively. Complex **2** has a 1-D chain and **3** is mononuclear.

## 2. Experimental

### 2.1. Materials and physical measurements

All reagents were used as purchased without further purification. IR spectra (KBr pellets) were recorded on a Perkin-Elmer spectrum One FT-IR spectrometer. The elemental analyses (EA) of C, H, N, and S were performed on a 2400 II, Perkin-Elmer elemental analyzer. X-ray powder diffraction intensities were measured with a Rigaku D/max-III A diffractometer (Cu-K $\alpha$ ,  $\lambda = 1.54056 \text{ \AA}$ ). CD spectra were measured on a JASCO J-810. Variable-temperature magnetic susceptibility data were obtained on polycrystalline samples using a Quantum Design MPMSXL7 SQUID magnetometer with an applied magnetic field of 1000 Oe from 2–300 K. TG-DTA tests were performed on a Perkin-Elmer thermal analyzer from room temperature to 1100 °C in a nitrogen atmosphere at a heating rate of 5 °C min<sup>-1</sup>.

### 2.2. Synthesis of $\{[Co(L)_2(H_2O)_3] \cdot H_2O\}_n$ (**1**)

To a methanol solution (20 mL) of HL (225 mg, 1 mmol) was added an aqueous solution (10 mL) of CoCl<sub>2</sub>·6H<sub>2</sub>O (119 mg, 0.5 mmol). When the pH of the solution was adjusted to 5.0–6.5 with Et<sub>3</sub>N (0.3–0.65 mL), the mixture was stirred at 60 °C for 2 h, then cooled to room temperature. The mixture was filtered and a light red solution was obtained. For crystallization, the solution remained undisturbed. After two weeks, pink block-shaped crystals were generated, washed with distilled water, and picked out after being dried in air. Yield: 217 mg [75% based on Co(II)]. Elemental analysis for C<sub>18</sub>H<sub>20</sub>CoN<sub>2</sub>O<sub>8</sub>S<sub>4</sub> (%): Calcd: C, 37.30; H, 3.49; N, 4.83; S, 22.13. Found: C, 37.16; H, 3.69; N, 4.97; S, 22.21. IR (KBr, cm<sup>-1</sup>): 3211s, 1589s, 1421s, 1309w, 1235w, 1007m, 746m, 720m, 673w.

### 2.3. Synthesis of $[Co(L)_2(H_2O)_2]_n$ (**2**)

The preparation of **2** was similar to that of **1**, except with pH of 4.0–5.0 with Et<sub>3</sub>N (0.2–0.3 mL), giving reddish needle-shaped crystalline products. Yield: 182 mg [67% based on Co(II)]. Elemental analysis for C<sub>18</sub>H<sub>16</sub>CoN<sub>2</sub>O<sub>6</sub>S<sub>4</sub> (%): Calcd: C, 39.77; H, 2.97; N, 5.16; S, 23.60. Found: C, 39.46; H, 2.79; N, 5.57; S, 23.68. IR (KBr, cm<sup>-1</sup>): 3187w, 2968m, 2921w, 1569s, 1430s, 1243m, 1007s, 750s, 723m, 686w.

### 2.4. Synthesis of $[Co(L)_2(H_2O)_4] \cdot 2H_2O$ (**3**)

The preparation of **3** was similar to that of **1**, except with pH of 3.0–4.0 with Et<sub>3</sub>N (1.5–0.2 mL), giving reddish rod-shaped crystalline products. Yield: 163 mg [53% based on

Table 1. Crystallographic data and structure refinement for **1–3**.

	<b>1</b>	<b>2</b>	<b>3</b>
Empirical formula	C <sub>18</sub> H <sub>20</sub> CoN <sub>2</sub> O <sub>8</sub> S <sub>4</sub>	C <sub>18</sub> H <sub>16</sub> CoN <sub>2</sub> O <sub>6</sub> S <sub>4</sub>	C <sub>18</sub> H <sub>24</sub> CoN <sub>2</sub> O <sub>10</sub> S <sub>4</sub>
Formula weight	579.53	543.50	615.56
Crystal system	Monoclinic	Monoclinic	Monoclinic
Space group	<i>P</i> 2 <sub>1</sub>	<i>C</i> 2/ <i>c</i>	<i>P</i> 2 <sub>1</sub> / <i>c</i>
<i>a</i> (Å)	8.2114(3)	34.246(5)	6.0557(2)
<i>b</i> (Å)	7.5866(3)	4.4484(6)	5.15872(15)
<i>c</i> (Å)	18.4644(7)	13.9243(18)	39.1082(12)
$\beta$ (°)	97.126(3)	94.829(12)	92.097(3)
Volume (Å <sup>3</sup> )	1141.39(8)	2113.7(5)	1220.91(7)
<i>Z</i>	2	4	2
<i>D</i> <sub>Calcd</sub> (Mg m <sup>-3</sup> )	1.686	1.708	1.674
<i>F</i> (0 0 0)	594	1108	634
$\theta$ range for data collection (°)	2.9–28.7	2.9–28.7	3.1–28.7
Reflections collected	12,434	7138	9864
Independent reflections	5014 [ <i>R</i> <sub>(int)</sub> = 0.029]	1897 [ <i>R</i> <sub>(int)</sub> = 0.112]	2493 [ <i>R</i> <sub>(int)</sub> = 0.031]
Goodness-of-fit on <i>F</i> <sup>2</sup>	1.05	1.18	1.14
Final <i>R</i> indices [ <i>I</i> > 2 $\sigma$ ( <i>I</i> )]	<i>R</i> <sub>1</sub> = 0.0297 $\omega R$ <sub>2</sub> = 0.0650	<i>R</i> <sub>1</sub> = 0.1078 $\omega R$ <sub>2</sub> = 0.2338	<i>R</i> <sub>1</sub> = 0.0418 $\omega R$ <sub>2</sub> = 0.0833
<i>R</i> indices (all data)	<i>R</i> <sub>1</sub> = 0.0371 $\omega R$ <sub>2</sub> = 0.0811	<i>R</i> <sub>1</sub> = 0.1643 $\omega R$ <sub>2</sub> = 0.2627	<i>R</i> <sub>1</sub> = 0.0496 $\omega R$ <sub>2</sub> = 0.0866
Flack parameter	0.018(13)		

Table 2. Selected bond lengths (Å) and angles (°) for **1–3**.

<b>1</b>					
Co1–O1	2.071(8)	Co1–O2A	2.109(2)	Co1–O3	2.094(2)
Co1–O5w	2.129(2)	Co1–O6w	2.097(2)	Co1–O7w	2.084(2)
O1–Co1–O2A	82.45(9)	O1–Co1–O3	89.95(8)	O1–Co1–O5w	96.68(9)
O1–Co1–O6w	93.10(8)	O1–Co1–O7w	172.17(9)	O2A–Co1–O5w	176.05(1)
O3–Co1–O2A	92.05(9)	O3–Co1–O5w	91.81(9)	O3–Co1–O6w	176.94(9)
O6w–Co1–O2A	88.76(9)	O6w–Co1–O5w	87.43(9)	O7w–Co1–O2A	89.96(9)
O7w–Co1–O3	88.39(8)	O7w–Co1–O5w	91.02(9)	O7w–Co1–O6w	88.64(8)
Symmetry code: A: $-x + 1, y - 1/2, -z + 1$					
<b>2</b>					
Co1–O1	2.123(7)	Co1–O2B	2.071(8)	Co1–O3w	2.101(9)
O2B–Co1–O1	88.8(3)	O2C–Co1–O1	91.2(3)	O2B–Co1–O3w	88.0(3)
O2C–Co1–O3w	92.0(3)	O3w–Co1–O1A	89.6(3)	O3w–Co1–O1	90.4(3)
Symmetry codes: A: $-x, -y + 2, -z + 1$ ; B: $x, y + 1, z$ ; C: $-x, -y + 1, -z + 1$					
<b>3</b>					
Co1–O1	2.092(8)	Co1–O3w	2.131(2)	Co1–O4w	2.070(2)
O1–Co1–O3w	95.26(8)	O1A–Co1–O3w	84.74(8)	O4wA–Co1–O1	88.76(7)
O4w–Co1–O1	91.24(7)	O4w–Co1–O3wA	90.78(8)	O4w–Co1–O3w	89.22(8)
Symmetry code: A: $-x + 2, -y + 1, -z$					

Co(II)]. Elemental analysis for C<sub>18</sub>H<sub>24</sub>CoN<sub>2</sub>O<sub>10</sub>S<sub>4</sub> (%): Calcd: C, 35.12; H, 3.94; N, 4.55; S, 20.83. Found: C, 35.46; H, 3.69; N, 4.47; S, 20.68. IR (KBr, cm<sup>-1</sup>): 3120<sub>w</sub>, 2968<sub>w</sub>, 1569<sub>s</sub>, 1428<sub>s</sub>, 1375<sub>s</sub>, 1232<sub>w</sub>, 1008<sub>m</sub>, 749<sub>m</sub>, 686<sub>w</sub>.

## 2.5. X-ray crystallographic determination

Single-crystal X-ray diffraction data of **1** were collected on a Bruker SMART CCD diffractometer by using graphite monochromated Mo-*K* $\alpha$  radiation ( $\lambda = 0.71073$  Å) at

Table 3. Hydrogen bond lengths (Å) and angles (°) in **1–3**.

$D-H\cdots A$	$D-H$	$H\cdots A$	$D\cdots A$	$D-H\cdots A$
<b>1</b>				
O5w–H5A $\cdots$ O3 <sup>#2</sup>	0.84	2.08	2.892 (3)	166
O5w–H5B $\cdots$ O8w	0.84	1.96	2.793 (3)	173
O6w–H6A $\cdots$ O8w <sup>#1</sup>	0.85	1.92	2.748 (3)	167
O7w–H7A $\cdots$ N1 <sup>#1</sup>	0.84	2.09	2.928 (3)	172
O7w–H7B $\cdots$ O4 <sup>#2</sup>	0.83	1.85	2.675 (3)	169
O8w–H8A $\cdots$ N2	0.84	2.03	2.841 (4)	161
O8w–H8B $\cdots$ O4 <sup>#3</sup>	0.84	2.02	2.856 (3)	170
Symmetry codes: #1: $-x + 1, y - 1/2, -z + 1$ ; #2: $-x + 2, y + 1/2, -z + 1$ ; #3: $x, y + 1, z$				
<b>2</b>				
O3w–H3A $\cdots$ O1 <sup>#1</sup>	0.85(8)	1.97(9)	2.755(12)	154(11)
O3w–H3B $\cdots$ N1	0.85(9)	2.11(10)	2.858(14)	147(8)
Symmetry code: #1: $x + 1/2, y + 3/2, z + 1$				
<b>3</b>				
O3w–H3A $\cdots$ O2	0.85(2)	1.99(3)	2.720(3)	144(2)
O4w–H4A $\cdots$ O1 <sup>#1</sup>	0.85(2)	2.01(2)	2.860(3)	176(2)
O4w–H4B $\cdots$ O5w	0.85(2)	1.83(2)	2.677(3)	175(2)
O5w–H5A $\cdots$ O2 <sup>#2</sup>	0.87(5)	2.08(5)	2.863(4)	150(4)
Symmetry codes: #1: $x, y + 1, z$ ; #2: $x - 1, y, z$				

room temperature. The data for **2** and **3** were collected at 293 K on an Agilent Technologies SuperNova diffractometer with Mo- $K\alpha$  radiation ( $\lambda = 0.71073$  Å). A semiempirical absorption correction using SADABS was applied, and the raw data frame integration was performed with SAINT [17]. Crystal structures were solved by the direct method using SHELXS-97 [18] and refined by full-matrix least-squares on all  $F^2$  data for the nonhydrogen atoms using SHELXL-97 [19] with anisotropic thermal parameters. All hydrogens were placed in calculated positions and refined isotropically, except hydrogens of water were located in a difference Fourier map and refined isotropically in the final refinement cycles. Details of crystallographic data are summarized in table 1. Selected bond lengths and angles for **1–3** are given in table 2 and hydrogen bond lengths and angles are listed in table 3.

### 3. Description of the crystal structures

#### 3.1. $\{[Co(L)_2(H_2O)_3]\cdot H_2O\}_n$ (**1**)

Single crystals of **1** were obtained, and its structure was resolved in the monoclinic space group  $P2_1$ . The structural analysis shows that **1** reveals a 1-D system with a mononuclear Co(II) unit. As illustrated in figure 1(a), the central cobalt Co1 is six-coordinate in a slightly distorted octahedron. The equatorial positions are composed by four carboxylate/water oxygens [O1, O2A, O5w and O7w, Co–O1 = 2.0718(1) Å, Co–O2A = 2.109(2) Å, Co–O5w = 2.129(2) Å and Co–O7w = 2.084(2) Å, symmetry code: A:  $-x + 1, y - 1/2, -z + 1$ ] and two carboxylate/water oxygens [O3 and O6w, Co–O3 = 2.094(2) Å and Co–O6w = 2.097(2) Å] occupy the axial position. The Co–O distances are similar to those for  $[Co(L')_2(H_2O)_2]_n \cdot 2nH_2O$  (HL' = 2-(6-oxo-6H-purin-1(9H)-yl) acetic acid; Co–O, 2.094

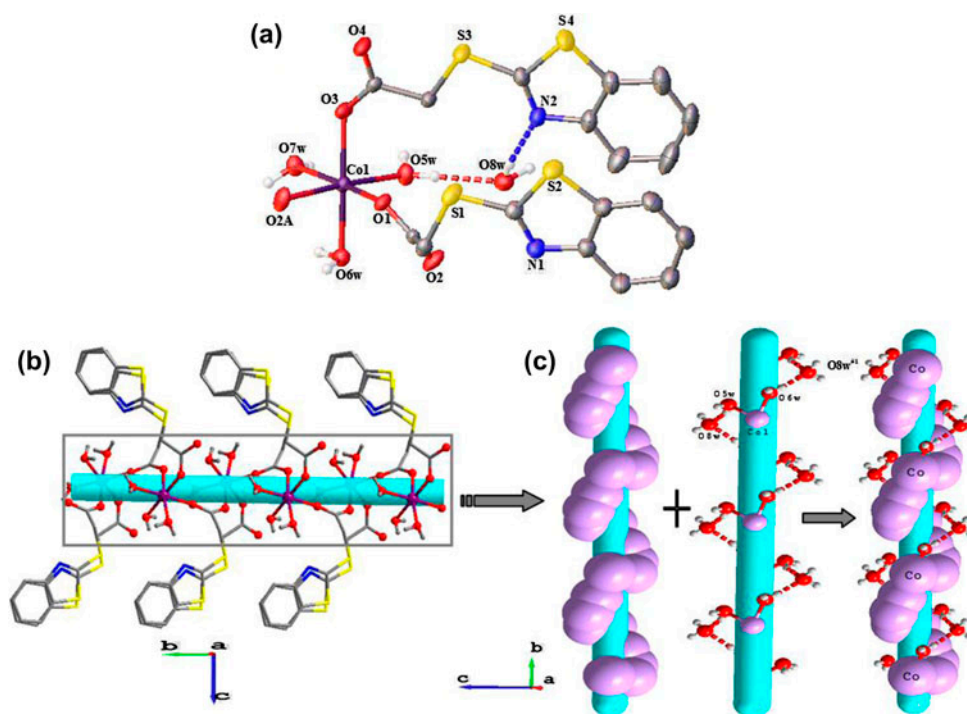


Figure 1. (a) The local coordination environment of Co(II) in **1** with 30% ellipsoid probability. Symmetry code: A:  $-x + 1, y - 1/2, -z + 1$ ; (b) A view of the 1-D helical chain of **1**; (c) The 1-D helical double chain of **1** composed by the helical Co–O–C–O chain and the helical metal–water chain. Symmetry code: #1:  $-x + 1, y - 1/2, -z + 1$ .

(4)–2.103(5) Å [20a] and  $\{[\text{Co}(3,4\text{-Hpdc})_2(\text{H}_2\text{O})_2] \cdot 2\text{H}_2\text{O} \cdot 2\text{dmsO}\}_n$  (3,4-Hpdc = 3,4-pyridinedicarboxylic acid; Co–O, 2.094(2)–2.166(2) Å [20b] and in the range of those for  $[\text{Co}_3(\text{EIDC})_2(\text{H}_2\text{O})_5]_n$  ( $\text{H}_3\text{EIDC}$  = 2-ethyl-1H-imidazole-4,5-dicarboxylic acid; Co–O, 1.984(7)–2.148(5) Å [20c]. Of the two carboxylate ligands, one is monodentate (O3), the other has *syn-anti* bridging (O1, O2) to connect adjacent Co(II) cations, forming a 1-D chain with  $2_1$  helicity along the *b* direction, in which the helical pitch is equal to the length of the *b*-axis [ $b = 7.593(4)$  Å], as shown in figure 1(b). The distance between the adjacent Co(II) centers connected by  $\text{L}^-$  is 5.126(5) Å; **1** is a helical chain furnished by carboxylate ligands.

Along the *b*-axis, we have also found a 1-D helical metal–water chain [21] comprised of Co(II), two coordinated waters (O5w and O6w), and a lattice water (O8w), linked by hydrogen bonds [O5w $\cdots$ O8w = 2.793(3) Å, O6w $\cdots$ O8w<sup>#1</sup> = 2.748(3) Å, symmetry code: #1:  $-x + 1, y - 1/2, -z + 1$ ] between water molecules [figure 1(c)]. The average O $\cdots$ O distance of the helical metal–water chain is 2.77 Å, which is slightly shorter than the reported 2.85 Å of liquid water [22] and 2.90 Å of a hexameric water cluster in  $\{[\text{Nd}(\text{p-HPIDC})(\text{ox})_{0.5}(\text{H}_2\text{O})] \cdot 2\text{H}_2\text{O}\}_n$  (p-H<sub>3</sub>PIDC = 2-(pyridinium-4-yl)-1H-imidazole-4,5-dicarboxylic acid, H<sub>2</sub>ox = oxalic acid; O1W $\cdots$ O2W = 2.911(5) Å, O2W $\cdots$ O3W<sup>#7</sup> = 2.893(7) Å, O3W<sup>#1</sup> $\cdots$ O2W = 2.912(7) Å; average, 2.90 Å) [23].



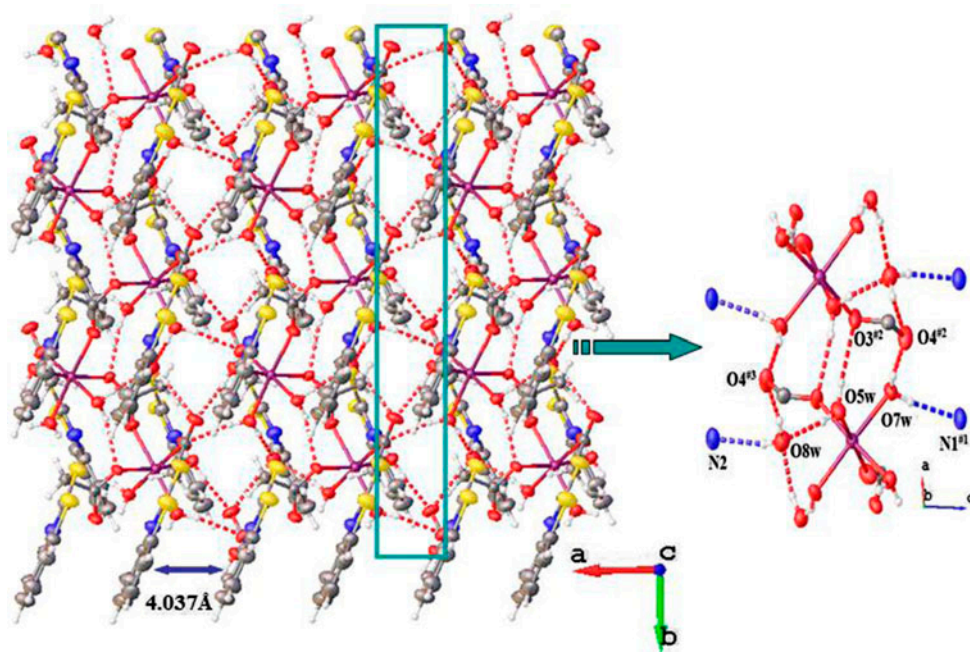


Figure 2. The 2-D supramolecular structure formed by hydrogen bonds and weak  $\pi \cdots \pi$  stacking interactions. Symmetry codes: #1:  $-x + 1, y - 1/2, -z + 1$ ; #2:  $-x + 2, y + 1/2, -z + 1$ ; #3:  $x, y + 1, z$ .

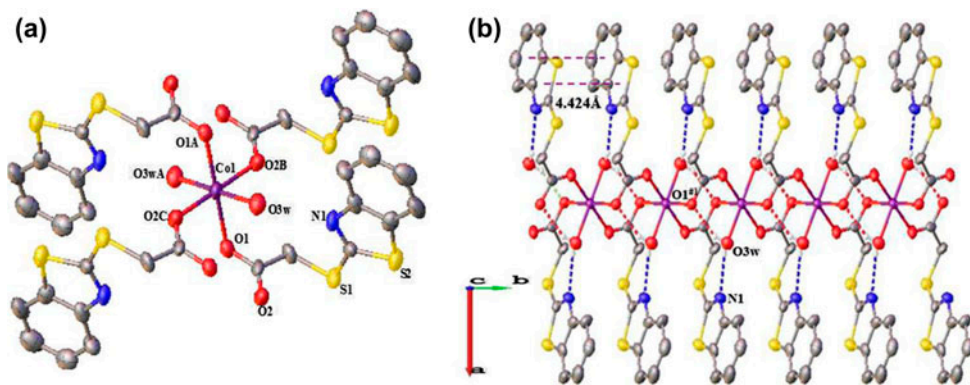


Figure 3. (a) The local coordination environment of Co(II) in **2** with 30% ellipsoid probability. Symmetry codes: A:  $-x, -y + 2, -z + 1$ ; B:  $x, y + 1, z$ ; C:  $-x, -y + 1, -z + 1$ ; (b) A view of the 1-D chain of **2** along the *b*-axis. Symmetry code: #1:  $x + 1/2, y + 3/2, z + 1$ .

Both helical chains are right-handed and they shared cobalt ions. That is, the 1-D system of **1** is a 1-D helical double chain arrangement joined by the coordination bonds of  $L^-$  and hydrogen bonds of the metal–water chain.

In this compound, weak  $\pi \cdots \pi$  stacking interactions exist with a centroid-to-centroid distance of 4.037 Å between benzene rings and thiazole rings of  $L^-$ , and abundant hydrogen bonds [ $O5w \cdots O3^{#2} = 2.892(3)$  Å,  $O7w \cdots N1^{#1} = 2.928(3)$  Å,  $O7w \cdots O4^{#2} = 2.675(3)$  Å,



$O8w \cdots N2 = 2.841(4) \text{ \AA}$ ,  $O8w \cdots O4^{#3} = 2.856(3) \text{ \AA}$ , average,  $2.84 \text{ \AA}$ , symmetry codes: #1:  $-x + 1, y - 1/2, -z + 1$ ; #2:  $-x + 2, y + 1/2, -z + 1$ ; #3:  $x, y + 1, z$ ] which connect not only the helical metal–water chains, but also the helical double chains to form a 2-D supramolecular structure along the  $a, b$  directions (figure 2).

### 3.2. $[Co(L)_2(H_2O)_2]_n$ (**2**)

Compound **2** belongs to the monoclinic  $C2/c$  space group and reveals a 1-D system with a mononuclear Co(II) unit. Co1 is six-coordinate and located on a crystallographic inversion center with a squashed octahedron coordination sphere [figure 3(a)]. Four carboxylate/water oxygens [O1, O1A, O3w, and O3wA, Co–O1 =  $2.123(7) \text{ \AA}$  and Co–O3w =  $2.123(7) \text{ \AA}$ , symmetry code: A:  $-x, -y + 2, -z + 1$ ] compose the equatorial positions and two carboxylate oxygens [O2B and O2C, Co–O2B =  $2.071(8) \text{ \AA}$ , symmetry codes: B:  $x, y + 1, z$ ; C:  $-x, -y + 1, -z + 1$ ] occupy axial positions. The Co–O distances are similar to those for  $[Co(II) L''(H_2O)]_n$  ( $H_2L'' = 2-(2-(3\text{-methyl-5-oxo-1-phenyl-1H-pyrazol-4(5H)-ylidene) hydrazinyl) benzoic acid$ ; Co–O,  $1.956(3)–2.111(3) \text{ \AA}$ ) [24a] and in the range of those for  $\{[Co(bdc)$

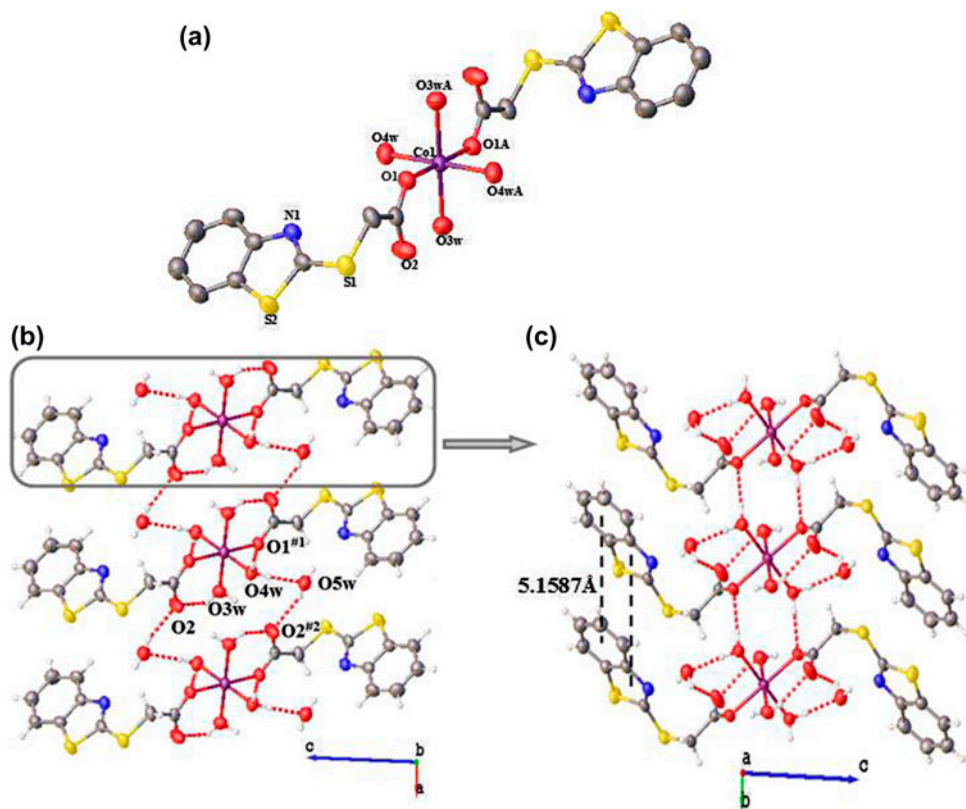


Figure 4. (a) The coordination environment of Co(II) in **3** with 30% ellipsoid probability. Symmetry code: A:  $-x + 2, -y + 1, -z$ ; (b) Adjacent cobalt units are connected by hydrogen bonds along the  $a$ -axis. Symmetry codes: #1:  $x, y + 1, z$ ; #2:  $x - 1, y, z$ ; (c) Adjacent cobalt units are connected by hydrogen bonds and very weak  $\pi \cdots \pi$  stacking interactions along the  $b$ -axis.

(bib)(H<sub>2</sub>O)]·H<sub>2</sub>O} <sub>n</sub> (H<sub>2</sub>bdc = 1,4-benzenedicarboxylic acid, bib = 1,4-bis(1-imidazolyl)benzene; Co–O, 2.042(3)–2.202(4) Å) [24b] and [Co<sub>1.5</sub>(tpa)<sub>2</sub>(N<sub>3</sub>)(H<sub>2</sub>O)] <sub>n</sub> (Htpa = *trans*-3-pyridylacrylic acid; Co–O, 2.032(8)–2.140(8) Å) [24c]. As shown in figure 3(b), along the *b*-axis, adjacent central cobalt ions are bridged by carboxyl groups of L<sup>−</sup> to furnish a 1-D chain. In this chain, two adjacent central cobalt ions are *syn-anti* bridged by two carboxyl groups of L<sup>−</sup> to form an eight-membered dicobaltacycle, in which the Co···Co distance is 4.448(5) Å (slightly shorter than the reported 4.518 Å of the eight-membered dicobaltacycle in [Co(mip)(bpa)] <sub>n</sub>, longer than 4.235 Å in [Co(mip)(bpp)] <sub>n</sub>, H<sub>2</sub>mip = 5-methylisophthalic acid, bpa = 1,2-bi(4-pyridyl)-ethane, bpp = 1,3-di(4-pyridyl)-propane) [25a], and slightly longer than 4.387(1) Å in [Co<sub>2</sub>(Hnbpdc)<sub>2</sub>(nbpdc)(bipy)<sub>2</sub>] <sub>n</sub>, H<sub>2</sub>nbpdc = 2-nitrobiphenyl-4,4'-dicarboxylic acid, bipy = 4,4'-bipyridine [25b]). Moreover, abundant hydrogen bonds [O3w···O1<sup>#1</sup> = 2.755(1) Å, O3w···N1 = 2.858(1) Å, average, 2.80 Å (slightly longer than 2.77 Å of **1** and shorter than the reported 2.85 Å of liquid water [22]), symmetry code: #1: *x* + 1/2, *y* + 3/2, *z* + 1] and weak π···π stacking interactions with a face-to-face distance of 4.424 Å between benzene rings and thiazole rings of L<sup>−</sup> ligands exist in the 1-D chain.

### 3.3. [Co(L)<sub>2</sub>(H<sub>2</sub>O)<sub>4</sub>]·2H<sub>2</sub>O (**3**)

As shown in figure 4(a), **3** consists of a centrosymmetric Co(II) unit. The Co1 is six-coordinate, showing an elongated octahedral environment, provided by four carboxylate/water oxygens [O1, O1A, O4w, and O4wA (symmetry code: A: *−x* + 2, *−y* + 1, *−z*), Co–O1 = 2.092(8) Å and Co–O4w = 2.070(2) Å] composing the equatorial plane and two water oxygens [O3w and O3wA, Co–O3w = 2.131(2) Å] occupying the axial positions. The Co–O distances are comparable to those for [Co(mbtx)(hpht)(H<sub>2</sub>O)] <sub>n</sub> (mbtx = 1,3-bis(1,2,4-triazol-1ylmethyl)benzene, H<sub>2</sub>hpht = homophthalic acid; Co–O, 2.064(4)–2.133(4) Å) [26a], and in the range of those for {[Co<sub>3</sub>(tm)<sub>2</sub>(3,4'-Hbpt)<sub>2</sub>(H<sub>2</sub>O)<sub>6</sub>]·2H<sub>2</sub>O} <sub>n</sub> (H<sub>3</sub>tm = trimellitic acid, 3,4'-Hbpt = 1H-3-(3-pyridyl)-5-(4-pyridyl)-1,2,4-triazole; Co–O, 2.048(3)–2.147(3) Å) [26b]. Unlike **1** and **2**, both carboxylate ligands in **3** are monodentate (O1, O1A). The adjacent cobalt units are connected by abundant hydrogen bonds along the *a*, *b* directions [O3w···O2 = 2.720(3) Å, O4w···O1<sup>#1</sup> = 2.860(3) Å, O4w···O5w = 2.677(3) Å, O5w···O2<sup>#2</sup> = 2.863(4) Å, average, 2.78 Å (slightly shorter than the reported 2.85 Å of liquid water [22]), symmetry codes: #1: *x*, *y* + 1, *z*; #2: *x* − 1, *y*, *z*] and very weak π···π stacking interactions (with a centroid-to-centroid distance of 5.1587 Å along the *b*-axis) between benzene rings and thiazole rings of L<sup>−</sup> [figure 4(b) and (c)].

## 4. Physical properties of 1–3

### 4.1. Powder X-ray diffraction

The experimental and simulated powder X-ray diffraction (PXRD) patterns of these complexes are shown in figure 5. In order to realize chiral symmetry breaking, eight parallel syntheses of **1** were carried out with pH in the range of 5.0–6.5. We can see that the measured PXRD patterns of the eight parallel bulk samples (b–i) are consistent with the calculated one, which can be concluded that they are all pure phase. For **2** and **3**, the measured PXRD patterns also agree with the corresponding calculated ones, and both of them are pure phase.

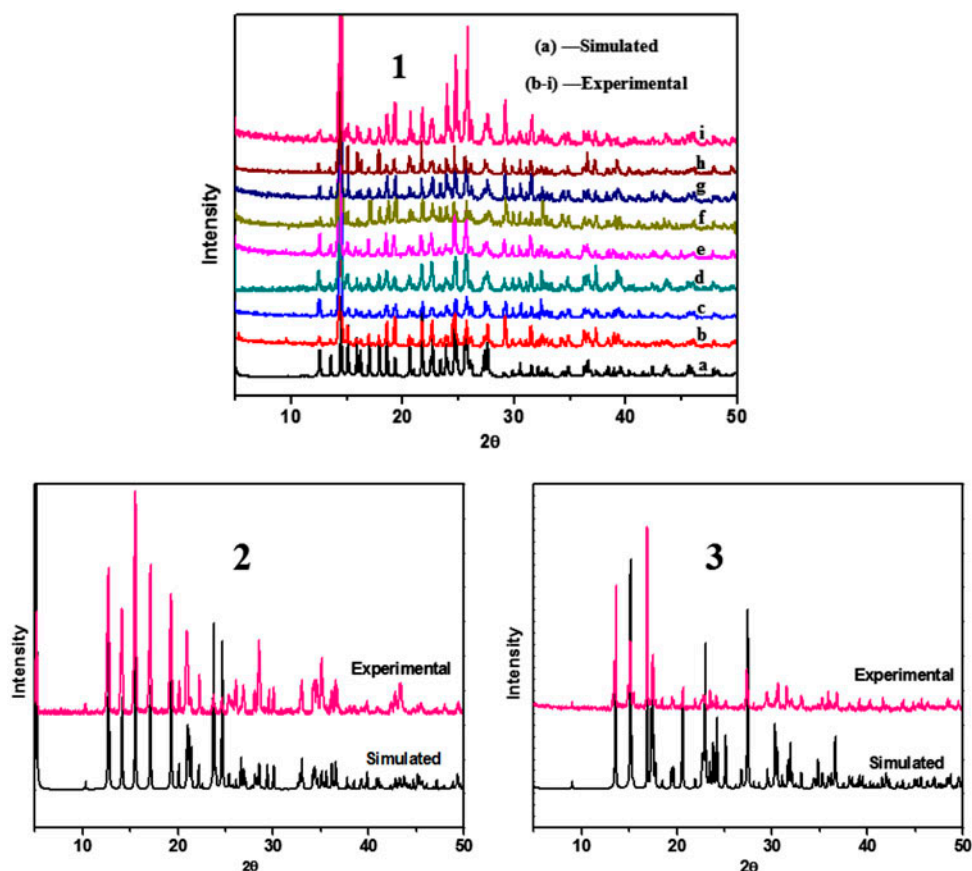


Figure 5. Measured and calculated powder X-ray diffraction (PXRD) patterns of 1–3 (b–i: the measured PXRD patterns for the eight batches of 1 in CD spectra).

#### 4.2. CD spectrum of 1

In order to evaluate the asymmetric crystallization of 1, CD spectra (figure 6) of bulk samples from eight parallel syntheses were measured in the solid state using a JASCO J-810 spectropolarimeter. Six bulk samples of 1 show a positive Cotton effect [27] at 508 nm, while two bulk samples of 1 exhibit the opposite CD signal at the same position. These results provide evidence for asymmetric crystallization. We attempted to control the law of chiral symmetry breaking by changing the pH of reaction, but we have not been able to find conditions that can reasonably regulate and control the law of helical chirality; unexpectedly, two different complexes, 2 and 3, were obtained.

#### 4.3. Magnetic properties of 1 and 2

The magnetic properties of 1 and 2 were carried out on crushed single crystals from 2.0 to 300.0 K at 1000 Oe, as shown in figure 7. For 1, the data above 35 K follow the Curie–Weiss law with  $C = 3.58 \text{ cm}^3 \text{ K mol}^{-1}$  and  $\theta = -20.63 \text{ K}$ . Above 40 K, the data of 2 also follow the Curie–Weiss law with  $C = 2.99 \text{ cm}^3 \text{ K mol}^{-1}$  and  $\theta = -28.00 \text{ K}$ . The magnetic

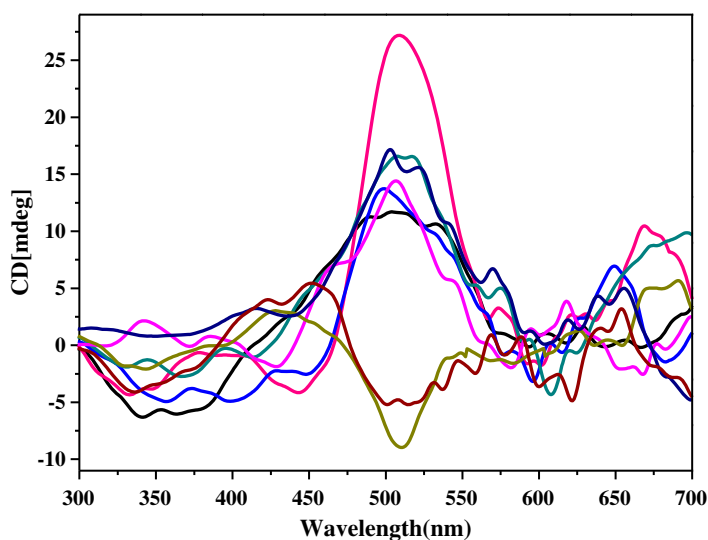


Figure 6. The solid-state CD spectra of **1** from eight batches.

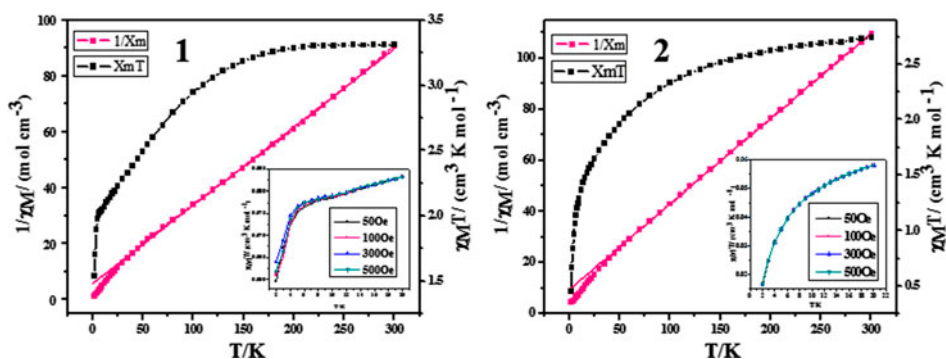


Figure 7. Plots of  $\chi_M T$  vs.  $T$  (black) and  $\chi_M^{-1}$  vs.  $T$  (red) for **1** and **2** (insets: plot of  $\chi_M T$  vs.  $T$  under different fields at low temperature) (see <http://dx.doi.org/10.1080/00958972.2015.1038996> for color version).

moments of **1** and **2** are similar at 300 K with  $\chi_M T$  of 3.31 and 2.74  $\text{cm}^3 \text{K mol}^{-1}$ , respectively, significantly larger than the theoretical spin-only value (1.88  $\text{cm}^3 \text{K mol}^{-1}$ ) for a magnetically active Co(II), which is common for high-spin octahedral Co(II) complexes because of the orbital contribution [28]. As  $T$  decreases,  $\chi_M T$  of **1** and **2** decrease continuously to a minimum value of 1.54 and 0.45  $\text{cm}^3 \text{K mol}^{-1}$  at 2 K, respectively. The global feature of them is characteristic of weak antiferromagnetic interactions. As shown in the crystallographic part, **1** and **2** are both made of Co(II) ions which are not only connected by *syn-anti* bridging of the carboxylate ligands, but also by weak intermolecular interactions to form a chain. Therefore, the overall antiferromagnetic interaction should be mainly attributed to magnetic exchange coupling within the Co–carboxylate chain. As illustrated in figure 7 (insets), the dependence of  $\chi_M T$  versus  $T$  curves of **1** and **2** at different fields is unobscured at low-temperature, which excludes spin canting.

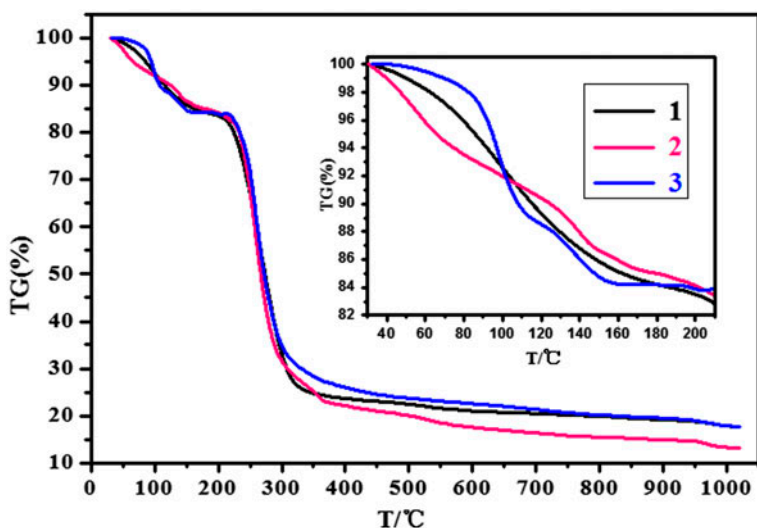


Figure 8. The TG curves of 1–3.

#### 4.4. Thermal stability of 1–3

The thermal stabilities of 1–3 have been investigated by thermogravimetric analysis (figure 8). The first weight loss of 12.69% of **1** from 70 to 137 °C corresponds to release of lattice and coordinated water (Calcd 12.42%). The second weight loss from 202 to 1000 °C is due to decomposition and combustion of the ligands and collapse of the framework. The final residual weight of 17.68% is consistent with that for  $\text{CoCO}_3$  (Calcd 20.52%) [29]. For **2**, the first weight loss of 6.41% at 98–164 °C corresponds to expulsion of coordinated water (Calcd 6.62%). The second weight loss of 79.96% which starts from 176 °C does not stop until heating and ends at 1000 °C corresponds to decomposition and combustion of the ligands (Calcd 82.42%). The final decomposition product (13.20%) is  $\text{CoO}$  (Calcd 13.79%) [20a, 30]. For **3**, the first weight loss of 5.97% at 50–96 °C corresponds to release of lattice water (Calcd 5.85%), the second weight loss of 10.34% from 98 to 202 °C corresponds to release of coordinated water (Calcd 11.70%), and further weight loss from 216 to 1000 °C is attributed to decomposition and combustion of the ligands and collapse of the framework. The remaining weight of 17.44% corresponds to formation of  $\text{CoCO}_3$  (Calcd 19.32%) [29].

## 5. Conclusion

We report three  $\text{Co(II)}$  complexes obtained under the same conditions except pH. Complex **1** was isolated at pH 5.0–6.5 and exhibits a rare chiral helical double chain structure, which achieved chiral asymmetry breaking through spontaneous asymmetric crystallization confirmed by CD spectra. Complex **2** was obtained at pH 4.0–5.0 and shows a 1-D chain structure. Complex **3** was generated at pH 3.0–4.0 and is a mononuclear structure. Chiral **1** can be generated from an achiral source without enantiopure additive; usually such compounds are synthesized by using enantiopure ligands [31]. Thus, conformation of the helical  $\text{Co-O-C-O}$  chain and the helical metal–water chain both play crucial roles in the chiral

generation. Only at pH 5.0–6.5 chiral **1** can be formed. The reason may be just like Wu *et al.* [15] said that a higher pH condition prompts Et<sub>3</sub>N to form [Co(Et<sub>3</sub>N)<sub>6</sub>]<sup>2+</sup> to compete with H<sub>2</sub>L for Co<sup>2+</sup> to control the kinetics of the target product crystallization. As a result, only a limited number of nuclei can be formed prior to crystal growth, and the probability of attaining only the left- or right-handed helical structure in these nuclei is greatly enhanced. The result shows that the pH of the reaction system is an important factor controlling the structures of target compounds. Magnetic studies revealed significant antiferromagnetic interaction between Co(II) ions in **1** and **2**. The exploration of the relationship between spontaneous asymmetry breaking and helicity could lead to new insights into the generation of helicity and homochirality in biopolymers.

### Disclosure statement

No potential conflict of interest was reported by the authors.

### Funding

This work was supported by National Natural Science Foundation of China [grant number 21101035], [grant number 21061002]; Guangxi Natural Science Foundation of China [grant number 2012GXNSFAA053035], [grant number 2012GXNSFBA053017]; Foundation of Key Laboratory for Chemistry and Molecular Engineering of Medicinal Resources.

### Supplementary data

Crystallographic data (excluding structure factors) for the structural analysis have been deposited with the Cambridge Crystallographic Data Center. CCDC reference numbers: 976441-976443 (1–3). These data can be obtained free of charge via [http://www.ccdc.cam.ac.uk/data\\_request/cif](http://www.ccdc.cam.ac.uk/data_request/cif).

### References

- [1] (a) C.M. Marson, C.J. Matthews, E. Yiannaki, S.J. Atkinson, P.E. Soden, L. Shukla, N. Lamadema, N.S.B. Thomas. *J. Med. Chem.*, **56**, 6156 (2013); (b) J.Z. Patel, T. Parkkari, T. Laitinen, A.A. Kaczor, S.M. Saario, J.R. Savinainen, D.N. Paldanius, M. Cipriano, J. Leppänen, I.O. Koshevoy, A. Poso, C.J. Fowler, J.T. Laitinen, T. Nevalainen. *J. Med. Chem.*, **56**, 8484 (2013); (c) V. Kumar, A.K. Banala, E.G. Garcia, J. Cao, T.M. Keck, A. Bonifazi, J.R. Deschamps, A.H. Newman. *ACS Med. Chem. Lett.*, **5**, 647 (2014); (d) M.H. Bolli, S. Abele, M. Birker, R. Bravo, D. Bur, R. de Kanter, C. Kohl, J. Grimont, P. Hess, C. Lescop, B. Mathys, C. Müller, O. Nayler, M. Rey, M. Scherz, G. Schmidt, J. Seifert, B. Steiner, J. Velker, T. Weller. *J. Med. Chem.*, **57**, 110 (2014).
- [2] (a) S. Pizzarello, A.L. Weber. *Science*, **303**, 1151 (2004); (b) P.-X. Yang, R.-F. Xu, S.C. Nanita, R.G. Cooks. *J. Am. Chem. Soc.*, **128**, 17074 (2006); (c) A. Kuzyk, R. Schreiber, Z.-Y. Fan, G. Pardatscher, E.M. Roller, A. Högele, F.C. Simmel, A.O. Govorov, T. Liedl. *Nature*, **483**, 311 (2012).
- [3] (a) D.K. Kondepudi, K.E. Crook. *Cryst. Growth Des.*, **5**, 2173 (2005); (b) T.J. Ward, B.A. Baker. *Anal. Chem.*, **80**, 4363 (2008); (c) R.E. Morris, X.-H. Bu. *Nat. Chem.*, **2**, 353 (2010).
- [4] (a) J.A. Switzer, H.M. Kothari, P. Poizot, S.-J. Nakanishi, E.W. Bohannon. *Nature*, **425**, 490 (2003); (b) T. Gibaud, E. Barry, M.J. Zakhary, M. Henglin, A. Ward, Y.-S. Yang, C. Berciu, R. Oldenbourg, M.F. Hagan, D. Nicastro, R.B. Meyer, Z. Dogic. *Nature*, **481**, 348 (2012); (c) P.A. Korevaar, S.J. George, A.J. Markvoort, M.M.J. Smulders, P.A.J. Hilbers, A.P.H.J. Schenning, T.F.A.D. Greef, E.W. Meijer. *Nature*, **481**, 492 (2012).
- [5] (a) T.J. Ward. *Anal. Chem.*, **78**, 3947 (2006); (b) A. Gabashvili, D.D. Medina, A. Gedanken, Y. Mastai. *J. Phys. Chem. B*, **111**, 11105 (2007); (c) S. Inagaki, J.Z. Min, T. Toyo'oka. *Anal. Chem.*, **80**, 1824 (2008); (d) Y.-Q. Tang, A.E. Cohen. *Science*, **15**, 333 (2011).



- [6] (a) V. Rauniyar, A.D. Lackner, G.L. Hamilton, F.D. Toste. *Science*, **334**, 1681 (2011); (b) Q.-X. Han, C. He, M. Zhao, B. Qi, J.-Y. Niu, C.-Y. Duan. *J. Am. Chem. Soc.*, **135**, 10186 (2013); (c) B.M. Trost, M. Rao, A.P. Dieskau. *J. Am. Chem. Soc.*, **135**, 18697 (2013); (d) I.E. Zoghbi, M. Kebdani, T.J.J. Whitehorne, F. Schaper. *Organometallics*, **32**, 6986 (2013); (e) M. Zhou, D.-J. Dong, B.-L. Zhu, H.-L. Geng, Y. Wang, X.-M. Zhang. *Org. Lett.*, **15**, 5524 (2013).
- [7] (a) C. Wang, T. Zhang, W.-B. Lin. *Chem. Rev.*, **112**, 1084 (2012); (b) P. Gerstel, S. Klumpp, F. Hennrich, A. Poschlad, V. Meded, E. Blasco, W. Wenzel, M.M. Kappes, C. Barner-Kowollik. *ACS Macro Lett.*, **3**, 10 (2013); (c) A.J. Gellman, Y. Huang, X. Feng, V.V. Pushkarev, B. Holsclaw, B.S. Mhatre. *J. Am. Chem. Soc.*, **135**, 19208 (2013).
- [8] (a) Y. Shoji, K. Tashiro, T. Aida. *J. Am. Chem. Soc.*, **128**, 10690 (2006); (b) M.M. Wanderley, C. Wang, C.-D. Wu, W.-B. Lin. *J. Am. Chem. Soc.*, **134**, 9050 (2012); (c) M. Iwamura, Y. Kimura, R. Miyamoto, K. Nozaki. *Inorg. Chem.*, **51**, 4094 (2012); (d) Y. Yang, X.-L. Pei, Q.-M. Wang. *J. Am. Chem. Soc.*, **135**, 16184 (2013); (e) K.W. Bentley, Y.G. Nam, J.M. Murphy, C. Wolf. *J. Am. Chem. Soc.*, **135**, 18052 (2013).
- [9] H.D. Flack. *Helv. Chim. Acta*, **86**, 905 (2003).
- [10] (a) D. Bradshaw, J.B. Claridge, E.J. Cussen, T.J. Prior, M.J. Rosseinsky. *Acc. Chem. Res.*, **38**, 273 (2005); (b) X.-L. Yang, M.-H. Xie, C. Zou, F.-F. Sun, C.-D. Wu. *CrystEngComm*, **13**, 1570 (2011); (c) L. Cheng, L.-M. Zhang, S.-H. Gou, Q.-N. Cao, J.-Q. Wang, L. Fang. *CrystEngComm*, **14**, 4437 (2012); (d) K.H. Park, T.H. Noh, Y.-B. Shim, O.-S. Jung. *Chem. Commun.*, **49**, 4000 (2013); (e) T. Shiga, M. Takeo, F. Iijima, G.N. Newton, H. Oshio. *New J. Chem.*, **38**, 1946 (2014).
- [11] (a) S. Supriya, S.K. Das. *Chem. Commun.*, **47**, 2062 (2011); (b) W.-X. Zheng, Y.-Q. Wei, X.-Y. Xiao, K.-C. Wu. *Dalton Trans.*, **41**, 3138 (2012); (c) C.K. Terajima, M. Ishii, T. Saito, C. Kanadani, T. Harada, R. Kuroda. *Inorg. Chem.*, **51**, 7502 (2012); (d) Q.-X. Yang, Z.-J. Chen, J.-S. Hu, Y. Hao, Y.-Z. Li, Q.-Y. Lua, H.-G. Zheng. *Chem. Commun.*, **49**, 3585 (2013); (e) H. Wang, Z. Chang, Y. Li, R.-M. Wen, X.-H. Bu. *Chem. Commun.*, **49**, 6659 (2013).
- [12] K.K. Bisht, E. Suresh. *Inorg. Chem.*, **51**, 9577 (2012).
- [13] D.B. Cline (Ed.). *Physical Origin of Homochirality in Life*, American Institute of Physics, New York, NY (1996).
- [14] D.K. Kondepudi, R.J. Kaufman, N. Singh. *Science*, **250**, 975 (1990).
- [15] S.-T. Wu, Y.-R. Wu, Q.-Q. Kang, H. Zhang, L.-S. Long, Z. Zheng, R.-B. Huang, L.-S. Zheng. *Angew. Chem. Int. Ed.*, **46**, 8475 (2007).
- [16] L. Qin, J.-S. Hu, M.-D. Zhang, Z.-J. Guo, H.-G. Zheng. *Chem. Commun.*, **48**, 10757 (2012).
- [17] Bruker AXS. *S.A.I.N.T. Software Reference Manual*, Madison, WI (1998).
- [18] G.M. Sheldrick. *Acta Crystallogr., Sect. A: Found. Crystallogr.*, **46**, 467 (1990).
- [19] G.M. Sheldrick, *SHELXS-97, Program for X-ray Crystal Structure Solution*, University of Göttingen, Göttingen, Germany (1997).
- [20] (a) X.-Q. Liu, Z.-Y. Li, X.-J. Yuan, B.-L. Wu. *J. Coord. Chem.*, **65**, 3721 (2012); (b) F.M. Scaldini, C.C. Corrêa, M.I. Yoshida, K. Krambrock, F.C. Machado. *J. Coord. Chem.*, **67**, 2967 (2014); (c) L. Sun, J.-F. Song, R.-S. Zhou, J. Zhang, L. Wang, K.-L. Cui, X.-Y. Xu. *J. Coord. Chem.*, **67**, 822 (2014).
- [21] G.A. Jeffrey. *An Introduction to Hydrogen Bonding*, p. 160, Springer, Oxford University Press, Oxford (1997).
- [22] D.S. Eisenberg, W. Kauzmann. *The Structure and Properties of Water*, Oxford University Press, New York, NY (1969).
- [23] N. Wang, X.-Y. Yu, X. Zhang, W.-P. Gao, R. Xin, H. Zhang, Y.-Y. Yang, X.-S. Qu. *J. Coord. Chem.*, **67**, 837 (2014).
- [24] (a) Y.-F. Qiao, L. Du, J. Zhou, Y. Hu, L. Li, B. Li, Q.-H. Zhao. *J. Coord. Chem.*, **67**, 2615 (2014); (b) K. Wang, E. Gao. *J. Coord. Chem.*, **67**, 563 (2014); (c) K.C. Mondal, O. Sengupta, M. Nethaji, P.S. Mukherjee. *Dalton Trans.*, 767 (2008).
- [25] (a) L.-F. Ma, X.-Q. Li, B. Liu, L.-Y. Wang, H.-W. Hou. *CrystEngComm*, **13**, 4973 (2011); (b) X.-H. Jing, X.-C. Yi, E.-Q. Gao, V.A. Blatov. *Dalton Trans.*, **41**, 14316 (2012).
- [26] J.-H. Zhou, Y. Wang, S.-N. Wang, T. Wang, Y.-C. Chen, G.-X. Liu. *J. Coord. Chem.*, **66**, 737 (2013); (b) F.-P. Huang, P.-F. Yao, W. Luo, H.-Y. Li, Q. Yu, H.-D. Bian, S.-P. Yan. *RSC Adv.*, **4**, 43641 (2014).
- [27] (a) G.-C. Ou, Z.-Z. Wang, L.-Z. Yang, C.-Y. Zhao, T.-B. Lu. *Dalton Trans.*, **39**, 4274 (2010); (b) Q.-X. Han, C. He, M. Zhao, B. Qi, J.-Y. Niu, C.-Y. Duan. *J. Am. Chem. Soc.*, **135**, 10186 (2013).
- [28] F.-P. Huang, Q. Zhang, Q. Yu, H.-D. Bian, H. Liang, S.-P. Yan, D.-Z. Liao, P. Cheng. *Cryst. Growth Des.*, **12**, 1890 (2012).
- [29] D.P. Martin, M.A. Braverman, R.L. LaDuca. *Cryst. Growth Des.*, **7**, 2609 (2007).
- [30] M.A. Nadeem, M. Bhadbhade, R. Bircher, J.A. Stride. *Cryst. Growth Des.*, **10**, 4063 (2010).
- [31] (a) L. Lin, R. Yu, W. Yang, X.-Y. Wu, C.-Z. Lu. *Cryst. Growth Des.*, **12**, 3304 (2012); (b) B. Wu, S. Wang, R. Wang, J. Xu, D. Yuan, H. Hou. *Cryst. Growth Des.*, **13**, 518 (2013).